J. Chem. Thermodynamics **1976**, 8, 471–491

Thermophysical measurements on transition-metal tungstates

II.[a] Heat capacities of antiferromagnetic nickel and cobalt tungstates[b]

CHRISTOPHER P. LANDEE and EDGAR F. WESTRUM, JR.[c]

Department of Chemistry, The University of Michigan, Ann Arbor, Michigan 48104, U.S.A.

(*Received 3 November 1975; in revised form 30 December 1975*)

The heat capacity of nickel tungstate ($NiWO_4$) was measured over the temperature range 5 to 350 K by adiabatic calorimetry, and that of cobalt tungstate ($CoWO_4$) from 5 to 550 K. Temperatures of maximum heat capacities for the antiferromagnetic anomalies in cobalt and nickel tungstates were (47.7±0.1) K and (59.80±0.05) K. Excess entropies associated with the antiferromagnetic anomalies were evaluated as $R \ln 2$ (1.38 $cal_{th}\ K^{-1}\ mol^{-1}$) for $CoWO_4$ and $R \ln 3$ (2.18 $cal_{th}\ K^{-1}\ mol^{-1}$) for $NiWO_4$ with the lattice heat capacities of the compounds approximated by that of $ZnWO_4$. In addition, the heat capacity of $CoWO_4$ showed a continuing excess heat capacity consistent with a Schottky anomaly from energy levels lying roughly 600 to 3400 $cal_{th}\ mol^{-1}$ above the ground state. Selected thermal functions: C_p°, S°, and $-\{G^\circ(T)-H^\circ(0)\}/T$ at 298.15 K are respectively 28.41, 30.08, and 14.01 $cal_{th}\ K^{-1}\ mol^{-1}$ for $CoWO_4$, and 27.77, 28.51, and 13.21 $cal_{th}\ K^{-1}\ mol^{-1}$ for $NiWO_4$.

Introduction

The first-row transition-element metal tungstates: $MnWO_4$, $FeWO_4$, $CoWO_4$, $NiWO_4$, and $ZnWO_4$, form an isostructural series of compounds in which the number of 3d electrons increases from 5 in $MnWO_4$ to 10 in $ZnWO_4$. The crystal structure of these compounds is of the $NiWO_4$-type,[1] space group $P2/c(C_{2h}^4)$ and the lattice parameters increase gradually (but irregularly) along the series.[2] Because the 3d shell is incomplete, $MnWO_4$, $FeWO_4$, $CoWO_4$, and $NiWO_4$ are paramagnetic at 300 K. At low temperatures, the compounds undergo cooperative transitions to antiferromagnetically-ordered states as shown by both magnetic susceptibility measurements[3–5] and magnetic structures determined by neutron diffraction.[6–8] $FeWO_4$, $CoWO_4$, and $NiWO_4$ share a common magnetic structure in which the moments lie in the *ac*-plane, inclined to the *a*-axis by angles of 29° for $FeWO_4$,[7] between 20 and 45° for $CoWO_4$,[8–10] and 15° for $NiWO_4$.[11] The magnetic cell is double the crystallographic unit cell along the *a*-axis with the two moments in each

[a] The previous paper in the series is reference 14.

[b] This work has been supported by the National Science Foundation, contracts NSF GP-33424X and NSF GP-42525X.

[c] To whom correspondence concerning this paper should be addressed.

cell parallel to one another and antiparallel to the pairs adjacent to them along the *a*-axis. This arrangement implies ferromagnetic layers within the chains in each *bc*-plane, coupled antiferromagnetically to the adjacent planes (compare figure 1). The magnetic space group (Shubnikov group) for this structure is P_c2/c. The more complicated magnetic structure of $MnWO_4$ is discussed by Dachs.[12]

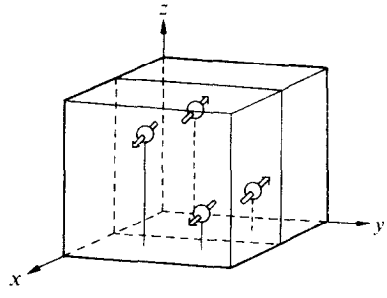

FIGURE 1. Magnetic structure of iron (II), nickel, and cobalt tungstates, after Ülkü.[7]

Measurement of the heat capacities of magnetic compounds yields valuable information concerning the magnetic disordering process as well as the magnetic entropy. The observed heat capacity is a combination of the magnetic disordering, of lattice vibrations, and—sometimes—of the population of nearby excited electronic states. To estimate the lattice contribution to the total heat capacity, the heat capacity of the isomorphous diamagnetic compound, $ZnWO_4$, is used.[13, 14]

Experimental

SAMPLE PREPARATION AND CHARACTERIZATION

Cobalt tungstate. The sample of cobalt tungstate purchased from Alfa Inorganics who had obtained it from Sylvania, Inc., was labelled "Crystal Grade", and had a stated purity of 99.96 moles per cent. The material was amorphous and showed no diffraction lines in preliminary X-rays analyses, but after firing in air at 1120 K for 20 h in a platinum crucible yielded a sharp X-ray pattern which revealed the presence of WO_3 impurity lines in addition to the $CoWO_4$ lines. Since WO_3 is soluble in alkali, the $CoWO_4$ was rinsed in 1 M KOH(aq), distilled water, then in 1 M HCl(aq) and again in water.† After drying in a drying oven, the sample was pressed to a pellet with 120 MPa pressure and fired for 30 h at 1275 K.

Since X-ray-diffraction analysis showed faint traces of WO_3 still present in the sample, the $CoWO_4$ was leached in 50 cm^3 batches in 400 cm^3 of 1 M KOH(aq) for 15 min. Each batch was then filtered, rinsed in distilled water, rinsed in 0.2 M HCl(aq) (to remove traces of alkali), and finally rinsed in distilled water. The sample was pelletted and fired as before. Subsequent X-ray-diffraction analyses showed no impurity lines and the lattice parameters derived for the $CoWO_4$ are in good accord

† Throughout this paper M = mol dm^{-3}; cal_{th} = 4.184 J; Torr = (101.325/760) kPa.

TABLE 1. Derived lattice parameters of cobalt tungstate

a/nm	b/nm	c/nm	β	Reference
0.467 ±0.001	0.569 ±0.001	0.494 ±0.001	90°	Broch[15]
0.4669±0.0003	0.5683±0.0003	0.4948±0.0003	90°	Swanson *et al.*[16]
0.4667±0.0001	0.5681±0.0001	0.4947±0.0001	90°	Sleight[2]
0.4666±0.0002	0.5680±0.0002	0.4948±0.0002	90°	This research (Guinier, Cu Kα)

with those of other investigators also given in table 1. Further details of the X-ray pattern obtained for both $CoWO_4$ and $NiWO_4$ are available elsewhere.[17]

The results of professional chemical analysis for cobalt and tungsten are listed in table 2 for two separate batches. Both the cobalt and tungsten are reported to be low with mole ratio n(Co)/n(W) of (0.978±0.020). If WO_3 were the only impurity present, the mole ratio would be low but the mass percentage of tungsten would exceed the theoretical value for cobalt tungstate, rather than be only 98.8 per cent

TABLE 2. Composition of transition metal tungstates, MWO_4: mass fraction f and amount of substance n

Compound and sample	$10^2 f$(M) [a]	$10^2 f$(W) [b]	n(M)/n(W)
$CoWO_4$-II′	18.7±0.03	59.2±0.3	0.986±0.02
$CoWO_4$-III′ [c]	18.6±0.3	59.2±0.3	0.978±0.02
Theoretical	19.21	59.90	1.000
$NiWO_4$	21.3±0.3 [d]	58.3±0.3 [d]	1.14 ±0.02
Theoretical	19.15	59.97	1.000

[a] Cationic metal by titration with EDTA.
[b] Spectrophometric determination for tungsten as tetrathiocyanato tungsten by the method of Gottschalk, *Z. Anal. Chem.* 1962, 187, 164.
[c] Calorimetric sample.
[d] Average of three determinations.

of theoretical. A composition of the form ($CoWO_4 + xWO_3 + y$), where y contains neither cobalt nor tungsten, would require 1.6 mass per cent of WO_3 and 1.8 mass per cent of y to duplicate the analytical results. The sensitivity of the X-ray analysis used is sufficient to rule out such a possibility, so the analytical results must be considered questionable.

To test for the possible presence of volatile impurities (water, etc.) a sample of several mg was heated to 1475 K under a nitrogen atmosphere in a Perkin-Elmer TGS-1 Thermobalance. No mass loss (±0.08) per cent was observed.

The presence of other metal impurities was tested in both batches II′ and III′ with a Perkin-Elmer 503 Atomic Absorption Spectrophotometer. Trace metals determined (mass fractions: 74×10^{-6} of cobalt, 524×10^{-6} of iron, 102×10^{-6} of

nickel, and 77×10^{-6} of zinc) yield an accumulated mass fraction of impurity less than 0.08 per cent so that compounds of these metals do not explain the discrepancy in the bulk analyses.

Atomic absorption spectroscopy was used to determine the mass percentage of cobalt in the sample. The reliability of this determination was low from background noise level within the instrument and problems of preparing consistent standards. Yet the analysis for cobalt gives (98.7 ± 0.8) mass per cent of the theoretical value. This value, when used with the commercially determined mass percentage of tungsten, gives $n(\mathrm{Co})/n(\mathrm{W}) = (1.00 \pm 0.01)$, close to unity.

Nickel tungstate. The sample of "Crystal Grade" nickel tungstate purchased from Alfa Inorganics had been manufactured by Sylvania, Inc. and had a reported purity of 99.96 moles per cent. When the sample was first investigated, it was a light-green amorphous powder. After annealing for 24 h at 1125 K the color changed to pea-green and X-ray exposure for 2 h revealed a pattern of sharp lines. Most lines could be indexed as $NiWO_4$ reflexions but three lines corresponded to reflexions from NiO.[18] A later exposure for 8 h on more sensitive Ilford Type-G film revealed the presence of additional impurity lines in the original material corresponding to reflexions from $CaWO_4$,[19] and from Na_2WO_4.[20] An additional NiO line appeared. However, the presence of the calcium tungstate and sodium tungstate were not known during the purification undertaken to remove the nickel oxide impurity.

The calorimetric sample of $NiWO_4$ was prepared in the following manner. The original material was pressed into a pellet, annealed overnight in a tube furnace at 1050 K, and then crushed in an agate mortar. The powder was poured into a ball mill, distilled water added to make a slurry, and the sample milled for 2 d to crush the powder. After removal from the mill and drying, the sample was forced through a 0.25 mm sieve, boiled for 15 min in 1 M HCl(aq) to leach out NiO. This acid wash changes the color of the sample from dark green to mustard yellow. The material was filtered, rinsed in distilled water, dried, and then given a final annealing at 1170 K for 14 h in a Vycor tube. The color of the sample changed to a dark gold during this annealing. A preliminary X-ray at this point showed the absence of all NiO lines, but very faint WO_3 lines persisted. Consequently, the material was boiled in 1 M KOH(aq), filtered, rinsed in distilled water, and dried.

Subsequently, X-ray studies yielded lattice parameters generated from the refined data shown in table 3 which agreed well with those of other investigators. Long-

TABLE 3. Derived lattice parameters of nickel tungstate

a/nm	b/nm	c/nm	β	Reference
0.469 ±0.001	0.567 ±0.001	0.494 ±0.001	90.33°	Broch[15]
0.460 ±0.0015	0.566 ±0.002	0.491 ±0.002	(90.08±0.08)°	Keeling[1]
0.4600±0.0004	0.5665±0.0004	0.4912±0.0004	90°	Swanson *et al.*[16]
0.4599±0.0001	0.5665±0.0001	0.4910±0.0001	90°	Sleight[2]
0.4600±0.0002	0.5663±0.0002	0.4911±0.0002	90°	This research (Guinier, Cu Kα)

exposure irradiations revealed three impurity lines but no NiO and WO_3 reflexions. Two of these are matched by lines of the α-cristobalite phase of SiO_2 which entered the sample during the final annealing in the Vycor tube. Where the sample had been in contact with the tube, a hard opaque coating formed which, when scraped from the inside of the tube and X-rayed, was observed to be pure α-cristobalite, evidently produced by mineralizing action of $NiWO_4$ on (amorphous) Vycor. The other impurity line is attributed to the persistent presence of calcium tungstate. The diminished relative abundance of the $CaWO_4$ in the final sample, as determined by the number and intensity of the X-ray reflexions observed, is attributed to the slight solubility in water of this contaminant and the frequent rinses in distilled water the sample received. The absence of sodium tungstate reflexions is consistent with its higher solubility in water.

The nickel tungstate sample was chemically analyzed for the presence of silicon, calcium, and sodium. The assumption that these contaminants are present as the following compounds, implies impurity levels of 0.56 mass per cent (2.80 moles per cent) of SiO_2, 0.20 mass per cent (0.21 mole per cent) of $CaWO_4$, and 0.08 mass per cent (0.08 mole per cent) of Na_2WO_4.

The results of chemical analysis for nickel and tungsten are listed in table 2. The value for nickel is high and that for tungsten is low; the calculated mole ratio $n(\mathrm{Ni})/n(\mathrm{W})$ is (1.14 ± 0.02). Since the X-ray-determined lattice parameters are in such good accord with the previously published values, and since the sensitivity of the X-ray technique is sufficiently great to determine the 0.2 mole per cent of $CaWO_4$ impurity, this anomalous $n(\mathrm{Ni})/n(\mathrm{W})$ mole ratio is not understood.

HEAT-CAPACITY MEASUREMENTS

Heat-capacity measurements in the range 5 to 350 K were made in the Mark II adiabatic cryostat[21] while those made in the 300 to 500 K range were made in the Mark IV adiabatic thermostat.[22] Relevant loading information for the samples is given in table 4.

TABLE 4. Calorimeter loading information: calorimeter volume V, sample mass m, pressure p of helium gas, and density ρ of the sample

[Torr = (101.325/760) kPa]

Compound	Calorimeter	V/cm³	m/g	p/Torr	ρ/g cm^{-3}
		Low-temperature Cryostat, Mark II			
$CoWO_4$	W-52	59.11	89.1043	63.0	7.76[a]
$NiWO_4$	W-30	18.88	43.7491	75.5	7.59
		Intermediate-temperature Thermostat, Mark IV			
$CoWO_4$	W-22-P	84.31	88.3598	55.0	7.76

[a] Compare reference 16.

Results

HEAT CAPACITIES

The heat capacities of $CoWO_4$ are given in table 5 in chronological sequence so that temperature increments used usually may be inferred from the temperature increments between adjacent determinations, and are expressed in terms of a molar mass

TABLE 5. Heat capacity of cobalt tungstate $CoWO_4$
($cal_{th} = 4.184$ J)

T/K	C_p/$cal_{th}\,K^{-1}\,mol^{-1}$	T/K	C_p/$cal_{th}\,K^{-1}\,mol^{-1}$	T/K	C_p/$cal_{th}\,K^{-1}\,mol^{-1}$	T/K	C_p/$cal_{th}\,K^{-1}\,mol^{-1}$
			Mark II Cryostat				
	Series I	303.06	28.62	12.62	0.139		Series VIII
92.84	10.76	313.15	29.04	13.87	0.194		See below
99.55	11.71	323.14	29.45	15.25	0.272		
113.17	13.58	333.14	29.85	16.88	0.371		Series IX
121.92	14.70	343.28	30.33	18.68	0.516	50.98	4.435
130.14	15.71					52.17	4.529
139.65	16.82		Series III		Series V	53.32	4.682
150.35	17.98	53.33	4.676	20.25	0.668	54.43	4.866
160.55	19.01	56.45	5.082	22.37	0.911	55.49	4.964
170.33	19.96	61.08	5.795	24.52	1.208	56.52	5.093
179.79	20.79	66.75	6.689	26.92	1.576	57.52	5.245
189.97	21.65	73.06	7.679	29.64	2.054	58.91	5.445
200.84	22.52	80.33	8.653	32.91	2.714	60.67	5.728
211.41	23.31			37.15	3.694	62.67	6.044
221.73	24.05		Series IV	41.43	4.838	64.88	6.388
231.81	24.71	4.885	0.008				
		5.652	0.010		Series VI		Series X
	Series II	6.329	0.011		See below	151.10	18.04
241.58	25.35	7.042	0.014			157.22	18.66
252.13	25.97	7.847	0.021		Series VII	162.21	19.15
262.48	26.59	8.626	0.032	34.22	2.996	163.97	19.31
272.67	27.13	9.452	0.051	37.23	3.711	167.87	19.69
282.72	27.67	10.40	0.075	40.32	4.524	171.70	20.08
292.84	28.16	11.46	0.097	42.91	5.303	176.42	20.47

T/K	ΔT/K	$\langle C_p \rangle$/$cal_{th}\,K^{-1}\,mol^{-1}$	C_p/$cal_{th}\,K^{-1}\,mol^{-1}$	T/K	ΔT/K	$\langle C_p \rangle$/$cal_{th}\,K^{-1}\,mol^{-1}$	C_p/$cal_{th}\,K^{-1}\,mol^{-1}$
		Series VI				Series XII	
45.50	4.42	6.424	6.332	43.31	0.87	5.432	5.438
50.95	6.48	4.711	4.442	44.17	0.83	5.738	5.742
				44.98	0.79	6.052	6.081
		Series VIII		45.75	0.75	6.469	6.454
45.16	2.09	6.175	6.170	46.23	0.21	6.608	6.703
47.12	1.84	7.147	7.302	46.44	0.20	6.644	6.831
49.21	2.34	4.666	4.482	46.64	0.20	7.055	6.954
				46.84	0.19	7.189	7.094
		Series XI		47.03	0.19	7.182	7.238
		Enthalpy detn. A		47.22	0.19	7.476	7.396
55.043	0.28	4.813	4.813	47.41	0.19	7.520	7.562

TABLE 5—*continued*

T/K	ΔT/K	$\langle C_p \rangle$ / cal$_{th}$ K^{-1} mol^{-1}	C_p / cal$_{th}$ K^{-1} mol^{-1}
		Series XII (cont.)	
47.60	0.18	7.738	7.744
47.79	0.19	7.062	7.180
47.99	0.20	6.431	6.037
48.21	0.23	5.248	5.413
48.45	0.23	5.165	5.010
48.69	0.25	4.734	4.743
48.94	0.25	4.562	4.581
49.20	0.25	4.417	4.483
49.45	0.25	4.438	4.424
49.71	0.25	4.370	4.382
49.97	0.25	4.378	4.381
50.22	0.25	4.367	4.387
50.48	0.25	4.417	4.414
50.73	0.25	4.428	4.426
50.98	0.25	4.452	4.436
		Series XIII	
43.19	0.88	5.403	5.400
43.96	0.65	5.662	5.667
44.60	0.62	5.936	5.919
45.22	0.60	6.257	6.197
45.81	0.58	6.473	6.483
46.25	0.31	6.717	6.722
46.51	0.20	6.839	6.873
46.71	0.20	7.057	7.003
46.91	0.20	7.179	7.148
47.11	0.19	7.328	7.300
47.30	0.19	7.468	7.466
47.44	0.09	7.814	7.592
47.53	0.09	7.711	7.678
47.62	0.09	7.592	7.771
47.72	0.09	7.655	7.820
47.81	0.10	7.008	6.988
47.92	0.11	6.377	6.387
48.08	0.22	5.914	5.814
48.31	0.24	5.241	5.248
48.55	0.25	4.871	4.871
48.80	0.25	4.658	4.862
49.05	0.26	4.507	4.531
49.31	0.26	4.355	4.451
49.57	0.26	4.473	4.402
49.83	0.26	4.318	4.377
50.09	0.26	4.384	4.383
		Series XIV	
47.24	0.17	7.369	7.412
47.37	0.10	7.797	7.542
47.47	0.10	7.771	7.619
47.57	0.10	7.603	7.708
47.66	0.10	7.796	7.802
47.76	0.10	7.497	7.700
47.86	0.11	6.670	7.650
47.97	0.11	6.408	6.272

Series XV
Enthalpy detn. B

T/K	C_p / cal$_{th}$ K^{-1} mol^{-1}	T/K	C_p / cal$_{th}$ K^{-1} mol^{-1}	T/K	C_p / cal$_{th}$ K^{-1} mol^{-1}	T/K	C_p / cal$_{th}$ K^{-1} mol^{-1}
			Mark IV Thermostat				
	Series I	320.23	29.41		Series VI	449.89	33.29
289.22	27.99	329.82	29.78	390.65	31.75	459.90	33.40
298.54	28.47	339.54	30.15	398.77	31.99	469.88	33.52
309.30	28.94	349.18	30.49	406.83	32.20	479.77	33.80
		359.29	30.80	414.86	32.39	489.64	34.00
	Series II	369.88	31.16	422.84	32.56	499.77	34.10
352.89	30.64	380.38	31.45	430.79	32.77	510.14	34.30
363.69	31.08			428.70	32.97	520.47	34.38
374.07	31.36		Series V	446.58	33.11	530.76	34.54
		352.85	30.61			541.00	34.70
	Series III	358.80	30.84		Series VII	551.18	34.85
410.63	32.24	365.70	31.14	332.16	29.82		
421.01	32.56	373.55	31.25	341.88	30.19		
		381.35	31.47				
	Series IV	389.11	31.68		Series VII		
311.10	29.00	396.83	31.92	439.82	33.00		

of 306.7808 g mol^{-1}; those for $NiWO_4$ are similarly given in table 6 and are expressed in terms of a molar mass of 306.5576 g mol^{-1}; the enthalpy determinations for both compounds are summarized in table 7. The molar heat capacities for both compounds together with revised values from the heat capacity of $ZnWO_4$ are presented in figure 2 (5 to 350 K) and figure 3 (300 to 550 K).

TABLE 6. Heat capacity of nickel tungstate $NiWO_4$
(cal_{th} = 4.184 J)

T/K	C_p/cal_{th} K^{-1} mol^{-1}	T/K	C_p/cal_{th} K^{-1} mol^{-1}	T/K	C_p/cal_{th} K^{-1} mol^{-1}	T/K	C_p/cal_{th} K^{-1} mol^{-1}
			Mark II Cryostat				
	Series I	246.57	24.89		Series X	33.141	2.235
107.22	11.42	256.71	25.50	6.348	0.013	37.062	2.971
113.83	12.30	266.67	26.10	7.468	0.060	41.151	3.713
123.38	13.51	276.48	26.66	7.986	0.043	45.809	4.686
133.41	14.72	286.14	27.17	8.748	0.073	50.340	5.755
143.70	15.94	295.90	27.66	9.783	0.082	52.926	6.426
153.47	17.00	305.74	28.11	10.998	0.093	Enthalpy detn. C	
163.32	18.03		Series III	12.030	0.123	66.647	6.288
173.85	19.09	63.25	6.156	13.057	0.169		
184.59	20.08	68.81	6.548	14.130	0.232		Series XI
194.98	20.99	75.44	7.299	15.439	0.300	293.85	27.58
205.07	21.83	83.21	8.361	16.877	0.391	303.90	28.07
214.91	22.61	92.07	9.540	18.468	0.511	314.22	28.53
224.95	23.36	102.26	10.86	20.224	0.666	324.44	28.95
235.21	24.08	112.65	12.20	22.145	0.851	334.54	29.41
				24.408	1.113	344.54	29.82
	Series II		Series IV to IX	26.850	1.424		
236.40	24.15		See below	29.598	1.809		

T/K	ΔT/K	$\langle C_p \rangle$/cal_{th} K^{-1} mol^{-1}	C_p/cal_{th} K^{-1} mol^{-1}	T/K	ΔT/K	$\langle C_p \rangle$/cal_{th} K^{-1} mol^{-1}	C_p/cal_{th} K^{-1} mol^{-1}
		Series IV		60.538	0.261	6.541	6.540
51.755	2.070	6.138	6.132	60.809	0.265	6.269	6.256
53.754	1.918	6.683	6.683	61.083	0.267	6.140	6.156
55.694	1.949	7.276	7.276	61.468	0.487	6.092	6.090
57.580	1.809	7.963	7.958	62.090	0.749	6.056	6.066
59.326	1.672	8.831	8.896				
61.141	1.947	6.343	6.146			Series VI	
63.091	1.938	6.082	6.078	55.464	1.937	7.194	7.200
				57.338	1.801	7.854	7.854
		Series V		58.415	0.339	8.320	8.309
52.097	2.186	6.214	6.231	58.757	0.334	8.501	8.483
54.203	2.014	6.809	6.820	59.032	0.205	8.631	8.631
56.153	1.872	7.412	7.428	59.240	0.202	8.788	8.811
57.970	1.750	8.141	8.118	59.446	0.199	9.047	9.050
59.016	0.325	8.658	8.636	59.649	0.196	9.243	9.240
59.344	0.318	8.904	8.906	59.850	0.195	9.294	—
59.664	0.311	9.221	9.256	60.059	0.205	8.440	8.281
59.984	0.317	8.868	8.860	60.279	0.223	7.170	7.082
60.275	0.249	7.200	7.080	60.514	0.232	6.597	6.524

TABLE 6—*continued*

T/K	ΔT/K	$\langle C_p \rangle$ / $cal_{th}\,K^{-1}\,mol^{-1}$	C_p / $cal_{th}\,K^{-1}\,mol^{-1}$
		Series VI (cont.)	
60.755	0.236	6.319	6.286
60.999	0.238	6.192	6.177
61.372	0.494	6.126	6.097
62.169	1.082	6.066	6.066
63.250	1.067	6.081	6.083
64.315	1.050	6.124	6.132
		Series VII	
54.596	0.370	6.882	6.936
		Enthalpy detn. A	
64.669	1.010	6.149	6.152
		Series VIII	
58.156	0.479	8.162	8.188
58.634	0.469	8.415	8.415
58.985	0.225	8.602	8.627
59.213	0.221	8.818	8.787
59.436	0.218	8.967	9.047
59.657	0.215	9.194	9.246
59.876	0.214	9.224	—
60.102	0.229	8.161	7.794
60,346	0.249	6.908	6.885
60.604	0.257	6.412	6.420
60.868	0.260	6.218	6.226
61.134	0.261	6.117	6.144
		Series IX	
50.864	0.971	5.901	5.901
51.815	0.917	6.138	6.156
		Enthalpy detn. B	
65.529	0.996	6.201	6.196

TABLE 7. Enthalpy determinations of cobalt and nickel tungstates, $CoWO_4$ and $NiWO_4$, in the Mark II cryostat

(cal_{th} = 4.184 J)

Determination	T_1/K	T_2/K	$H(T_2)-H(T_1)$ / $cal_{th}\,mol^{-1}$	$H(55\,K)-H(35\,K)$ / $cal_{th}\,mol^{-1}$
		$CoWO_4$ in Mark II Cryostat		
A (Series XI)	32.66	54.90	104.43	98.10
B (Series XV)	35.88	54.55	92.96	98.02
Series VII, VIII, and IX	35.54	54.97	96.04	98.04
Series XII	42.88	51.11	46.48	98.04
			Mean:	(98.05±0.06)

Determination	T_1/K	T_2/K	$H(T_2)-H(T_1)$ / $cal_{th}\,mol^{-1}$	$H(65\,K)-H(45\,K)$ / $cal_{th}\,mol^{-1}$
		$NiWO_4$ in Mark II Cryostat		
A (Series VII)	54.78	64.16	67.88	128.93
B (Series IX)	52.28	65.02	89.85	128.94
C (Series X)	53.37	66.03	88.82	128.68
Series V	51.00	62.47	81.681	128.65
			Mean:	(128.80±0.28)

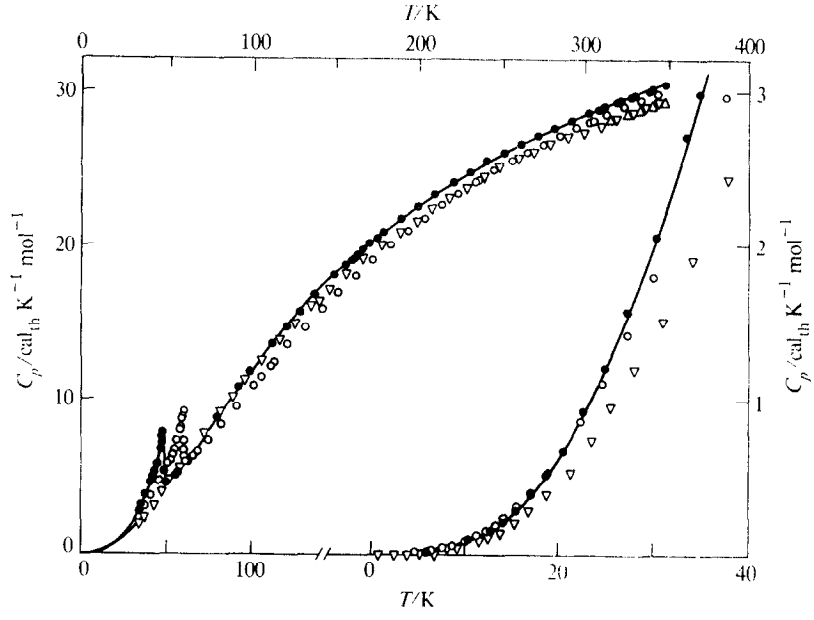

FIGURE 2. Heat capacities of zinc, nickel, and cobalt tungstates, 5 to 350 K. ●, $CoWO_4$ (Mark II results); ○, $NiWO_4$ (Mark II results); △, $ZnWO_4$ (Mark II results); ▲, $ZnWO_4$ (Mark IV results).

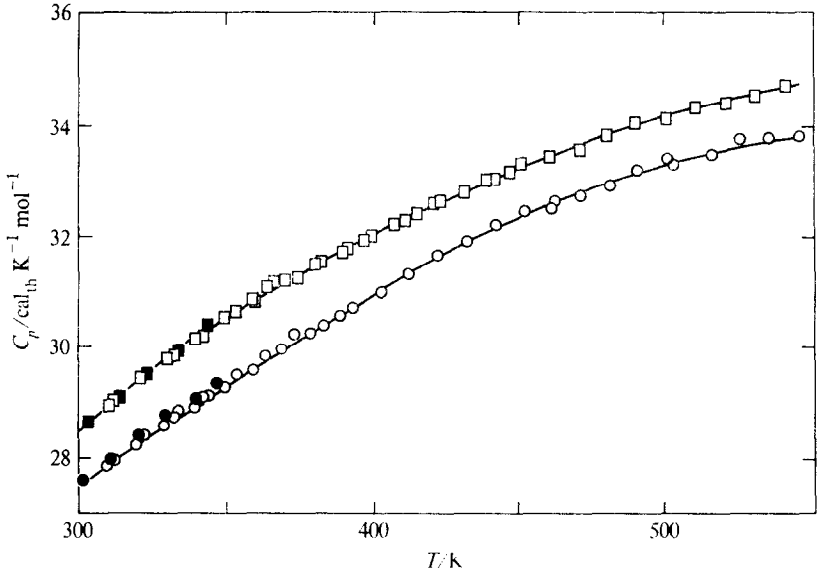

FIGURE 3. Heat capacities of zinc and cobalt tungstates, 300 to 550 K. ■, $CoWO_4$ (Mark II results); □, $CoWO_4$ (Mark IV results); ●, $ZnWO_4$ (Mark II results); ○, $ZnWO_4$ (Mark IV results).

ADJUSTMENT FOR IMPURITIES

The presence of the separate phase impurities in the nickel tungstate necessitated adjustment of the results in terms of the enthalpies of α-cristobalite and calcium tungstate. The thermal functions for silicon dioxide used in the analysis were generated by curve fitting the low-temperature, 5 to 300 K, heat capacities of Westrum[23] which had been extrapolated to 350 K. The adjustment for SiO_2 amounted to about 1 per cent below 10 K and about 0.5 per cent over the rest of the temperature region measured. The thermal functions for calcium tungstate used in the analysis for nickel tungstate were generated from the polynomial representation of the low-temperature heat capacities of Lyon and Westrum.[24] The adjustment for separate-phase calcium tungstate was less than 0.1 per cent of the molar heat capacity. Since the mole percentage of the sodium tungstate impurity phase was so low and since data for this compound are available only above 50 K,[25] no adjustment was made to the heat capacity of nickel tungstate for the sodium tungstate phase. Preliminary corrections showed the correction for sodium tungstate to amount to less than 0.05 per cent in regions where reasonable estimates could be made for the heat capacity of sodium tungstate.

THERMOPHYSICAL FUNCTIONS

The experimental molar heat capacities for both samples in non-transition regions (nickel tungstate adjusted for impurities) were fitted to polynomials in temperature by the method of least squares, and integrated to yield values of the thermophysical functions at selected temperature intervals. These derived values are presented in tables 8 and 9 for cobalt and nickel tungstates. Within the transition regions the thermal functions are based upon numerical integration of heat-capacity points mapped on large scale plots.

TABLE 8. Thermophysical functions of cobalt tungstate $CoWO_4$
($cal_{th} = 4.184$ J)

T / K	C_p / $cal_{th}\ K^{-1}\ mol^{-1}$	$\{S°(T)-S°(0)\}$ / $cal_{th}\ K^{-1}\ mol^{-1}$	$H°(T)-H°(0)$ / $cal_{th}\ mol^{-1}$	$-\{G°(T)-H°(0)\}/T$ / $cal_{th}\ K^{-1}\ mol^{-1}$
5	0.005	(0.003)	(0.012)	(0.001)
10	0.061	0.016	0.122	0.004
15	0.253	0.072	0.843	0.016
20	0.642	0.193	2.982	0.044
25	1.275	0.400	7.676	0.093
30	2.124	0.704	16.09	0.168
35	3.176	1.108	29.25	0.272
40	4.435	1.612	48.19	0.407
45	6.094	2.223	74.20	
50	4.380	2.858	104.24	
60	5.623	3.752	153.31	1.194
70	7.189	4.737	217.58	1.628
80	8.783	5.800	297.39	2.083
90	10.328	6.925	393.02	2.558
100	11.790	8.089	503.7	3.052

TABLE 8—*continued*

T / K	C_p / $cal_{th}\ K^{-1}\ mol^{-1}$	$\{S°(T)-S°(0)\}$ / $cal_{th}\ K^{-1}\ mol^{-1}$	$H°(T)-H°(0)$ / $cal_{th}\ mol^{-1}$	$-\{G°(T)-H°(0)\}/T$ / $cal_{th}\ K^{-1}\ mol^{-1}$
110	13.170	9.278	628.6	3.564
120	14.471	10.481	766.8	4.090
130	15.69	11.688	917.7	4.628
140	16.85	12.893	1080.5	5.176
150	17.93	14.093	1254.4	5.730
160	18.94	15.28	1438.8	6.290
170	19.90	16.46	1633.1	6.854
180	20.80	17.62	1836.7	7.420
190	21.65	18.77	2049.0	7.987
200	22.46	19.90	2269.6	8.555
210	23.21	21.02	2498.0	9.122
220	23.93	22.11	2733.7	9.687
230	24.61	23.19	2976.4	10.251
240	25.25	24.25	3225.7	10.813
250	25.86	25.30	3481.3	11.371
260	26.44	26.32	3742.8	11.926
270	26.99	27.33	4010.0	12.478
280	27.52	28.32	4282.5	13.026
290	28.02	29.30	4560.2	13.571
300	28.50	30.25	4842.8	14.111
310	28.95	31.20	5130	14.647
320	29.38	32.12	5422	15.18
330	29.78	33.03	5718	15.71
340	30.16	33.93	6017	16.23
350	30.52	34.81	6321	16.75
360	30.86	35.67	6628	17.26
370	31.17	37.52	6938	17.77
380	31.47	37.36	7251	18.27
390	31.75	38.18	7567	18.77
400	32.02	38.98	7886	19.27
410	32.27	39.78	8208	19.76
420	32.52	40.56	8531	20.25
430	32.75	41.33	8858	20.73
440	32.98	42.08	9187	21.20
450	33.20	42.83	9517	21.68
460	33.41	43.56	9851	22.14
470	33.61	44.28	10186	22.61
480	33.80	44.99	10523	23.07
490	33.97	45.69	10862	23.52
500	34.12	46.37	11202	23.97
510	34.26	47.05	11544	24.42
520	34.40	47.72	11887	24.86
530	34.53	48.38	12232	25.30
540	34.68	49.02	12578	25.73
550	34.82	49.66	12925	26.16
273.15	27.16	27.64	4095.2	12.651
298.15	28.41	30.08	4790.2	14.011

TABLE 9. Thermophysical functions of nickel tungstate $NiWO_4$
($cal_{th} = 4.184$ J)

T / K	C_p / $cal_{th}\,K^{-1}\,mol^{-1}$	$\{S°(T)-S°(0)\}$ / $cal_{th}\,K^{-1}\,mol^{-1}$	$H°(T)-H°(0)$ / $cal_{th}\,mol^{-1}$	$-\{G°(T)-H°(0)\}/T$ / $cal_{th}\,K^{-1}\,mol^{-1}$
5	0.010	(0.003)	(0.012)	(0.001)
10	0.079	0.026	0.198	0.007
15	0.273	0.090	1.014	0.022
20	0.643	0.215	3.228	0.053
25	1.187	0.414	7.739	0.104
30	1.861	0.688	15.32	0.178
35	2.628	1.032	26.50	0.274
40	3.497	1.438	41.77	0.394
45	4.505	1.907	61.71	0.535
50	5.672	2.440	87.08	0.699
60	8.604	3.740	158.8	
70	6.655	4.717	222.2	1.541
80	7.886	5.683	294.7	1.998
90	9.241	6.690	380.3	2.463
100	10.568	7.733	479.4	2.938
110	11.843	8.800	591.6	3.422
120	13.079	9.884	716.2	3.915
130	14.289	10.978	853.1	4.416
140	15.47	12.081	1001.9	4.925
150	16.61	13.188	1162.4	5.438
160	17.70	14.295	1334.0	5.957
170	18.73	15.40	1516.2	6.480
180	19.68	16.50	1708.3	7.006
190	20.57	17.59	1909.7	7.535
200	21.41	18.66	2119.7	8.064
210	22.21	19.73	2337.8	8.594
220	22.97	20.78	2563.7	9.124
230	23.70	21.81	2797.1	9.653
240	24.41	22.84	3037.7	10.181
250	25.09	23.85	3285.2	10.708
260	25.72	24.85	3539.3	11.233
270	26.31	25.83	3799.5	11.755
280	26.86	26.79	4065.4	12.275
290	27.37	27.75	4336.6	12.792
300	27.86	28.68	4612.8	13.306
310	28.34	29.60	4893.7	13.817
320	28.81	30.51	5179	14.325
330	29.27	31.40	5470	14.829
340	29.71	32.28	5765	15.33
350	30.13	33.15	6064	15.83
273.15	26.49	26.13	3882.7	11.919
298.15	27.77	28.51	4561.3	13.211

The estimated error in the thermodynamic functions of cobalt tungstate is less than 0.1 per cent above 100 K. The error for the thermodynamic functions of nickel tungstate is larger, due to the uncertainty in the mass fractions of the impurity phases. Since the accumulative correction to the molar heat capacity is less than 0.6 per cent, the uncertainty in the thermal functions is still less than 0.2 per cent above 100 K.

The values of the entropy and enthalpy at the lowest temperatures in parentheses in the tables of thermal functions were obtained from plots of C_p/T against T^2. For either compound, the magnitude of this extrapolation is negligible. The entropies and Gibbs energies have not been adjusted for nuclear spin or for isotopic mixing contributions and, hence, are practical values for use in chemical thermodynamic calculations.

Discussion

SUPEREXCHANGE INTERACTIONS

As a consequence of the intensive study of magnetic interactions in insulators, semi-empirical rules, the Goodenough-Kanamori rules (clearly formulated in reviews by Anderson)[26, 27] have been developed for predicting the sign of the interaction through which magnetic ions couple their moments. When cations occupy octahedral holes in closest-packed anion lattices, *e.g.* for tungstates and dichlorides,[28] the cation–anion–cation angle is 90° and the Goodenough-Kanamori rules predict antiferromagnetic exchange for the iron(II), cobalt, and nickel compounds (compare Goodenough[29]). The iron(II), cobalt, and nickel tungstates (and dichlorides) are antiferromagnets in which the spins are ferromagnetically aligned within each layer and the spins in neighboring layers are aligned antiferromagnetically.[30] In $MnWO_4$ (and $MnCl_2$), however, the cations do not order ferromagnetically[31] within each layer.

Detailed superexchange paths in the tungstates were first discussed by Van Uitert *et al.*[3] The structure of the tungstates can be thought of as a (distorted) hexagonal closest-packed array of oxygens with the tungsten and metal ions in the octahedral holes, forming independent zigzag chains along the *c*-axis of the crystal.[32] Each W-octahedral chain is attached by common corners to four M-chains and each M-chain is also surrounded by four W-chains. Each M^{2+} ion can interact by 90° superexchange with its two nearest neighbors in the chain, with which it shares two oxygen atoms each. There is also the possibility of next-nearest neighbor exchange within the chains, involving the tungsten atoms in an adjacent octahedron. Inter-chain coupling is possible both between layers and within the same layer by exchange paths of the type M–O–W–O–M, where all the angles involved are close to 90°. These interlayer interactions should be large, since the results of Lesne and Caillet[33] predict that the strongest bonding paths are between layers. Since the exchange interaction is enhanced with bond strength, the interlayer exchange interaction should be significant. Superexchange interactions of the type M–O–W–O–M have been studied in the ordered perovskites by Blasse[34] and found to be comparable in strength to those in the tungstates.

MAGNETIC BEHAVIOR

Susceptibilities of the tungstates[3–5] show characteristic maxima associated with antiferromagnetic phase changes. Since magnetic moments of the iron, cobalt, and nickel ions are all in excess of expectation for a spin-only model, considerable orbital angular momentum is retained by the ions within their low-symmetry crystal fields. Calculations predicting the amount retained involve lengthy considerations of the low-symmetry distortions of the octahedral fields and the magnitudes of the spin–orbit coupling. Cobalt tungstate is the only tungstate for which this calculation has been done. The authors, Zvyagin and Khats'ko,[9] were able to calculate susceptibilities and magnetic moments from their assigned energy levels in good accord with their experimental values.

Also significant is the discrepancy between the paramagnetic Curie temperatures Θ_p derived from susceptibility measurements in the low-temperature region and the high-temperature (290 to 700 K) measurements of Shapovalova *et al.*[4] which yield positive Θ_p's for ferrous and cobalt tungstate. These positive Θ_p's are indicative of ferromagnetic interactions within the crystal, even though the materials are known to be antiferromagnetic. Since in cobalt and iron(II) tungstate the ions in the *bc* plane are aligned ferromagnetically, with adjacent planes aligned antiferromagnetically, the high-temperature determination of susceptibility may reflect the dominance of the intralayer exchange. This type of behavior is known to exist in the transition-metal dichlorides where adjacent planes of ferromagnetic ions are aligned antiferromagnetically. The strong intralayer ferromagnetic interaction leads to positive paramagnetic Curie temperatures even at low temperatures. As pointed out by Dachs,[12] molecular-field theory leads to the relation:

$$|\Theta|_p/T_n = \Sigma J_{ij}/\Sigma J_{ij} S_i \cdot S_j.$$

In $MnWO_4$, the near-neighbor antiferromagnetic coupling leads to the cancellation of terms in the denominator, producing a large ratio (5.5). The ferromagnetic planes in the $FeWO_4$, $CoWO_4$, and $NiWO_4$ do not produce such cancellations and the ratios are significantly lower, (0.3, 1.8, and 0.8, respectively).

SPECIAL INFORMATION

Several investigations have been made of the electronic energy levels of pure and of doped diamagnetic tungstates. Study of the latter was undertaken with the intention of eliminating exchange effects.

In studies on the pure tungstates, Ferguson and others[35, 36] measured the absorption spectra of $CoWO_4$ and $NiWO_4$.

As discussed by Lyon,[37] the crystal-field splittings are 25 and 18 per cent less for the Co^{2+} and Ni^{2+} ions in the tungstate than when they are octahedrally coordinated in the diamagnetic oxide MgO.[35, 36] Such a decrease is sufficient to alter the expected colors of the samples. Whereas octahedrally coordinated cobalt and nickel compounds in solution are usually pink and green, the respective tungstates are blue and mustard yellow. These decreases in crystal-field splitting are attributed to the electron-withdrawing power of the W^{6+} ion, as mentioned by Lyon[37] and

also by Shannon and Vincent[38] in their discussion of covalency in the tungstates. This large effect by the tungsten ion makes the superexchange path involving the tungsten important.

The optical absorption spectra of Ni^{2+} ion in $ZnWO_4$ has been studied by Reynolds *et al.*[39] In an octahedral field the ground state of Ni^{2+} is a singlet, which will not split under a crystal field of lower symmetry. Reynolds *et al.* found this $^3A_2$ term to lie more than 6000 cm^{-1} below the first excited $^3T_2(E)$ term. Still, the spin–orbit coupling in the nickel ion must reintroduce orbital angular momentum into the ground states, since the effective magnetic moments exceed the spin-only prediction. However, no information is available as regards these energy states.

The assignment of the lowest levels for Co^{2+} ions in diamagnetic tungstate matrices has been accomplished by Atsarkin *et al.*[40] for $Co^{2+}:MgWO_4$, and by Zvyagin and Khats'ko,[41] and by Bates and co-workers,[42] for $Co^{2+}:ZnWO_4$. Atsarkin *et al.* measured the optical absorption spectra of the cobalt ions in $MgWO_4$ (0.01 mass per cent of Co^{2+}) at 300 K. They were able to interpret the spectra observed without considering either the orthorhombic components of the crystal field or the non-centrosymmetric location of the cobalt ions. They used the crystal-field parameters derived from the spectra to calculate the splitting of the lowest triplet state into six Kramers doublets by the spin–orbit interaction. Zvyagin and Khats'ko use the results of e.p.r. studies of $Co^{2+}:ZnWO_4$ as well as their own measurements of the single-crystal magnetic susceptibilities to assign energy levels to the six Kramers doublets. The agreement with the results of Atsarkin *et al.* is reasonable. Bates *et al.* have also studied the e.p.r. spectrum of $Co^{2+}:ZnWO_4$ and assigned energies to the six doublets on the basis of their results. The agreement with the results of Zvyagin and Khats'ko is excellent.

An additional estimate of the wavenumber interval Δ separating the ground-state doublet from the first excited doublet of Co^{2+} in $ZnWO_4$ has been given by Galkin *et al.*[43] They interpret their measurements of the broadening of the e.p.r. line in terms of spin–lattice relation times with a value $\Delta = (230 \pm 30)$ cm^{-1}.

SCHOTTKY ANOMALIES AND MAGNETIC TRANSFORMATION

Using the standard formulas for heat capacity as a function of energy levels,[44] it is possible to calculate the expected Schottky-type behavior in the heat capacity of cobalt tungstate. Beginning at about 60 K, the heat capacity should rise to a maximum of about 1.35 $cal_{th}\ K^{-1}\ mol^{-1}$ at a temperature of 200 K, then drop 10 per cent by 300 K, after which it should slowly rise towards the maximum as the temperature increases beyond 500 K.

Since the ground state of nickel tungstate is an orbital singlet, the magnetic entropy to be obtained will simply be $R \ln(2S+1) = R \ln 3$. At the transition temperature of cobalt tungstate (for which only the lowest Kramers doublet is thermally populated) the expected entropy change associated with the antiferromagnetic ordering would be $R \ln 2$ similar to the behavior of cobalt in CoF_2 and $CoCl_2$.[45] In addition, there should be further contributions to the entropy attributed to the population of the higher-lying doublets.

RESOLUTION OF MAGNETIC AND LATTICE CONTRIBUTIONS

In the preliminary step, the Debye characteristic temperatures Θ_D were calculated for each experimental point for tungstate including zinc tungstate.[14] The curve for Θ_D of zinc tungstate behaves normally. The other two curves have regions where the values are anomalously low; these correspond to the regions of large magnetic contributions to the heat capacity. Ratios of the Θ_D's: $\Theta_D(CoWO_4)/\Theta_D(ZnWO_4)$ and $\Theta_D(NiWO_4)/\Theta_D(ZnWO_4)$ were calculated as a function of temperature. For these compounds, the ratios below 100 K reflect the magnetic contributions to the heat capacity.

Assessment of the low-temperature Θ_D, and subsequently the low-temperature heat capacity, involves a complication due to the presence of the excited state in the cobalt ion because the Schottky contributions to the heat capacity of cobalt tungstate lower the observed Θ_D's. To determine the lattice heat capacity, Schottky heat capacities were generated from the spectroscopic data of Co^{2+} ions in $MgWO_4$ ($Co^{2+}:MgWO_4$) and Co^{2+} ions in $ZnWO_4$ ($Co^{2+}:ZnWO_4$). These heat capacities were then subtracted from the experimental heat capacities and the Θ_D's calculated for the resulting values. Since the harmonic approximation predicts $\Theta_D(CoWO_4)/\Theta_D(ZnWO_4) = \{M(Zn)/M(Co)\}^{1/2} = 1.053$, the estimated curve was drawn to this value as a lower limit. The molar masses of the ions rather than of the molecules were used since the heavy tungsten atoms form a matrix in which the first-row metals oscillate. Such behavior has been seen in the studies of iron impurities in metal host lattices.[46] Additional evidence for such a limit is the valence-force-field calculation of Lesne and Caillet[33] which showed the strongest bonds within the crystal were between W and O; the metal ions are bound relatively weakly to the oxygens. Hence, at temperatures greater than 100 K, the estimated curve was smoothly interpolated between the two calculated curves.

$NiWO_4$

A simple mass adjustment of Θ_D does not suffice for a lattice estimate of nickel tungstate. As can be seen in figure 2, above 60 K, the heat capacity of zinc tungstate is greater than that of nickel tungstate. A mass adjustment does little to this difference.

Similar behavior has been seen previously in the study of the metal difluorides by Stout and Catalano.[47] When the heat capacity of ZnF_2 is simply subtracted from that of NiF_2, the remaining heat capacity is significantly negative for several hundred kelvins. Stout and Catalano[47] assumed the vibrational contributions to the entropy and heat capacity of the difluorides obey a law of corresponding states, scaling as the parameter (T/T_m), where T_m is the melting temperature. Such an assumption was necessary to take proper account of the large differences between the melting temperatures of the zinc and nickel difluorides.

Since the reported melting temperatures of $NiWO_4$: 1663 K,[1] 1723 K,[48] are higher than that of $ZnWO_4$: 1474 K[48, 49] and of all other tungstates, the lattice estimate must take the melting-temperature differences into consideration. The relation chosen between the Θ_D of nickel and zinc tungstates was the Lindemann melting formula[50] which indicates the melting temperature T_m to be proportional

to such structural factors as ionic masses, sizes of unit cell, and Θ_D each to appropriate powers:

$$T_m \propto \Theta_D^2 V^{2/3} M,$$

The low-temperature limit of the ratio of the Θ_D's of nickel and zinc tungstate was then taken as

$$\Theta_D(NiWO_4)/\Theta_D(ZnWO_4) = [T_m(Ni)\{V(Zn)\}^{2/3}M(Zn)/T_m(Zn)\{V(Ni)\}^{2/3}M(Ni)]^{1/2} = 1.133.$$

The lowest limit was then joined to the experimental ratio of the ratio $\Theta_D(NiWO_4)/\Theta_D(ZnWO_4)$ at 150 K. The estimated $\Theta_D(NiWO_4)$ lattice heat capacities were then calculated from the Debye equation and the estimated Debye Θ_D's.

EXCESS HEAT CAPACITIES OF $NiWO_4$ AND $CoWO_4$

The heat capacities of these tungstates and the estimated lattice heat capacities in the vicinity of the transition temperatures are shown in figure 4 together with the

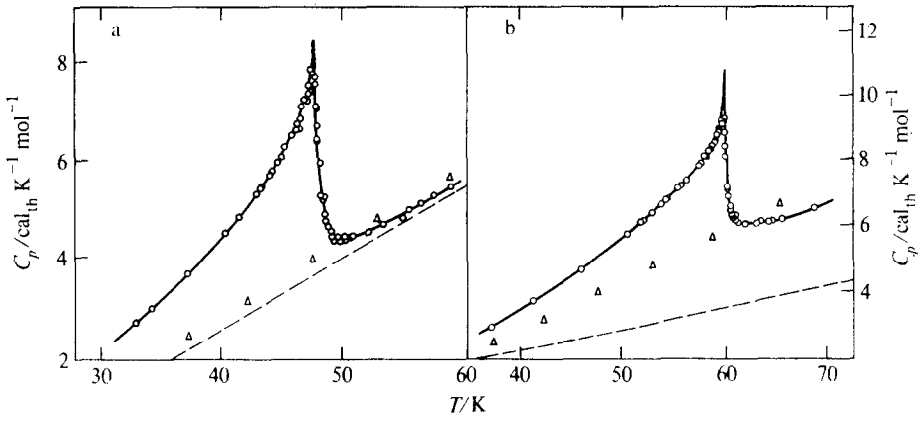

FIGURE 4. (a), (b). Heat capacities in the transition region—(a) for cobalt tungstate and (b) for nickel tungstate. ○, experimental values for $NiWO_4$ and $CoWO_4$; △, those for $ZnWO_4$; the dashed curve is the adopted lattice contribution.

zinc tungstate values used for comparison with the lattice contribution. To determine the excess entropies and enthalpies, the differences between the pairs of curves were integrated. The resulting entropy and enthalpy of transition for nickel tungstate are

$$\Delta S_{mag} = 2.06 \text{ cal}_{th} \text{ K}^{-1} \text{ mol}^{-1}, \qquad \Delta H_{mag} = 100.2 \text{ cal}_{th} \text{ mol}^{-1}.$$

A graph of magnetic entropy for nickel tungstate is shown in figure 5(a). The entropy obtained corresponds to 94 per cent of $R \ln 3$.

The existence of a discrepancy between the expected and experimental entropies cannot be considered surprising, in view of the crudeness of the lattice approximation. Even assuming the Lindemann melting relation to be valid, the Θ_D ratio curve chosen

was selected as reasonable, but is certainly not definitive. One indication of probable error in the assignment of the lattice is the fraction of entropy appearing above the Néel temperature. In three-dimensional magnetic systems, this entropy is often greater than 30 per cent of the total and continues to appear at $3T_N$. For the nickel

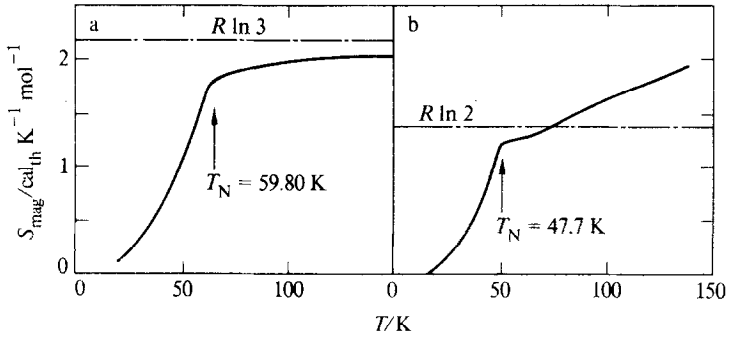

FIGURE 5. (a), (b) Magnetic entropies of (a) nickel tungstate and (b) cobalt tungstate.

tungstate only 18 per cent appears above T_N. However, within the uncertainties present, the total entropy is considered as evidence for the expected spin-disorder transition in nickel tungstate.

The excess entropy and enthalpy of cobalt tungstate were calculated from the difference of the total and estimated lattice curves shown in figure 4(b) on which the heat capacity of zinc tungstate is also shown. The excess entropy is displayed in figure 5(b). The entropy approaches $R \ln 2$; then the Schottky contribution to the heat capacity causes the entropy to rise again. Nevertheless, the magnetic entropy associated with the antiferromagnetic transition is clearly $R \ln 2$, not the $R \ln 4$ predicted from the spin-only model. The entropy above T_N, associated with magnetic short-range order, cannot be directly evaluated but the difference between $R \ln 2$ and the entropy which has appeared by T_N is 23 per cent of $R \ln 2$.

The excess heat capacities of cobalt and nickel tungstates show antiferromagnetic spin-wave contributions at low temperatures, as can be seen in figure 6. From considerations of mass and volume, the lattice heat capacities of nickel and cobalt tungstate should be *lower* than the heat capacity of zinc tungstate. The fact that the heat capacities are larger, while still proportional to T^3, demonstrates the existence of spin-wave heat capacities for these compounds. Interestingly enough, nickel tungstate has the same initial slope as cobalt tungstate even though its transition temperature is 13 K higher.

Although iron(II), cobalt, and nickel tungstates consist of ferromagnetic layers aligned antiferromagnetically, there is no evidence for two-dimensional magnetic behavior in the tungstates. In K_2NiF_4,[51] K_2MnF_4,[52] and $MnTiO_3$,[53, 54] anomalies in the susceptibilities have been interpreted as indicative of two-dimensional ordering, *e.g.* more than 45 per cent of the magnetic entropy of $MnTiO_3$ appears above the Néel temperature. However, these three compounds all display antiferromagnetic

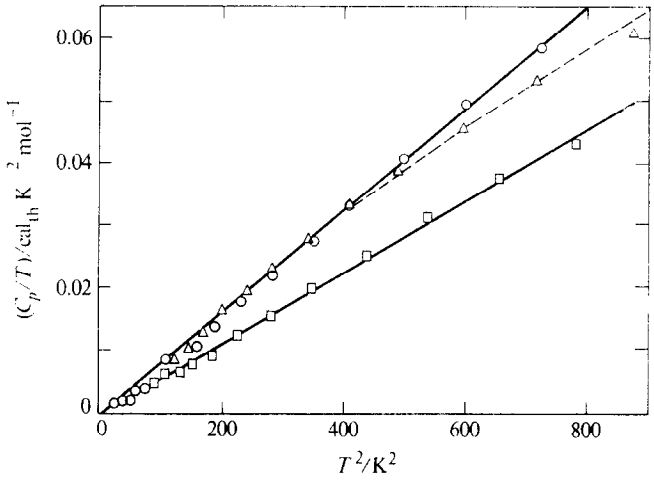

FIGURE 6. Plot of C_p/T against T^2 for: ○, cobalt tungstate; □, nickel tungstate; △, zinc tungstate.

coupling within the layers, unlike the $FeWO_4$, $CoWO_4$, and $NiWO_4$. The absence of such characteristic behavior in the susceptibilities of any of the tungstates and the relatively low percentages of short-range entropy herald essentially three-dimensional exchange properties.

REFERENCES

1. Keeling, R. O. *Acta. Cryst.* **1957,** 10, 209.
2. Sleight, A. W. *Acta. Cryst.* Section B, **1972,** 28, 2899.
3. Van Uitert, L. G.; Sherwood, R. C.; Williams, H. J.; Rubin, J. J.; Bonner, W. A. *J. Phys. Chem. Solids* **1964,** 25, 1447.
4. Shapovalova, R. D.; Belova, V. I.; Zalesskii, A. D.; Gerassimov, Ya. I. *Russ. J. Phys. Chem.* **1961,** 35, 1340.
5. Weitzel, H. *Neus Jahrb. Mineral. Abhand.* **1970,** 113, 13.
6. Dachs, H.; Weitzel, H.; Stull, E. *Solid State Commun.* **1966,** 4, 473.
7. Ülkü, D. *Zeit. Fur Krist.* **1967,** 124, 192.
8. Weitzel, H. *Solid State Commun.* **1970,** 8, 2071.
9. Zvyagin, A. I.: Khats'ko, E. N. *Soviet Physics—Solid State* **1970,** 12, 258.
10. Gredescul, V. M.; Greduscul, S. A ; Eremenko, V. V.; Naukemko, V. M. *J. Phys. Chem. Solids* **1972,** 33, 859.
11. Eremenko, V. V. Personal communication (1975).
12. Dachs, H. *Solid State Commun.* **1969,** 7, 1015.
13. Lyon, W. G.; Westrum, E. F., Jr. *J. Chem. Thermodynamics* **1974,** 6, 781.
14. Landee, C. P.; Westrum, E. F., Jr. *J. Chem. Thermodynamics* **1975,** 7, 973.
15. Broch, E. K. *Norske Videnskaps—Acad. Skriften I.* No. 8, **1929,** 61 pp.
16. Swansen, H. E.; Morris, M. C.; Stinchfield, R. P.; Evans, E. E. *Natl. Bur. Stds.* (U.S.), Monograph 26, Sec. 6.2, **1963.**
17. Landee, C. P., Ph-D. Thesis, The University of Michigan, Ann Arbor, Michigan 1975. *Diss. Abs.* **1975,** 36, 75-29272. Detailed supplementary information on X-ray structural patterns for some samples and detailed thermodynamic functions for all samples are presented in an NAPS document No. 02765 for 22 pages of supplementary material. Order from ASIS/NAPS c/o Microfiche Publications, 440 Park Avenue South, New York, N.Y. 10016 U.S.A. Remit in advance for each NAPS accession number. Make checks payable to Microfiche Publications. Photocopies are $5.50. Microfiche are $3.00. Outside of the U.S. and Canada, postage is $2.00 for a photocopy or $1.00 for a fiche.

18. Powder Data File, Joint Committee on Powder Diffraction Standards, 1845 Walnut Street, Philadelphia, Pennsylvania 19103, U.S.A. Card No. 4-0835.
19. Reference 18. Card No. 7-210.
20. Reference 18. Card No. 92-772.
21. Westrum, E. F., Jr.; Furukawa, G. T.; McCullough, J. P. Adiabatic low-temperature calorimetry in *Experimental Thermodynamics*, Vol. I. McCullough, J. P.; Scott, D. W., editors. Butterworths: London, **1968.**
22. West, E. D.; Westrum, E. F., Jr. Adiabatic calorimetry from 300 to 800 K". in *Experimental Thermodynamics*, Vol. I. McCullough, J. P.; Scott, D. W., editors. Butterworths: London, **1968.**
23. Westrum, E. F., Jr., Unpublished results.
24. Lyon, W. G.; Westrum, E. F., Jr. *J. Chem. Thermodynamics* **1968,** 49, 3374.
25. King, E. G.; Weller, W. W. *U.S. Bur. Mines Rept. Invest.*, No. 5791, **1961.**
26. Anderson, P. W. Theory of magnetic exchange interactions: exchange in insulators and semiconductors. In *Solid State Physics.* Seitz, F.; Turnbull, D., editors. Academic Press: New York. **1963.**
27. Anderson, P. W. Exchange in insulators: superexchange, direct exchange, and double exchange. In *Magnetism*, Vol. 1. Rado, G. T.; Suhl, H., editors. Academic Press: New York. **1963.**
28. Grime, H.; Santos, J. A. *Z. Kristallogs. Mineral.* **1934,** 88, 136.
29. Goodenough, J. B. *Magnetism and the Chemical Bond.* Interscience: New York. **1963.**
30. Wilkinson, M. K.; Cable, J. W.; Wollan, E. O.; Koehler, W. C. *Phys. Rev.* **1959,** 113, 497.
31. Wilkinson, M. K.; Cable, J. W.; Wollan, E. O.; Koehler, W. C. *Oak Ridge National Laboratory Report* ORNL-2501, **1958** (unpublished); Oak Ridge National Laboratory Report ORNL-2430. **1959** (unpublished).
32. Cid-Dresdner, H.; Escobar, C. *Z. Kristallogr. Mineral* **1968,** 127, 61.
33. Lesne, J. P.; Caillet, P. *Can. J. Spect.* **1973,** 18, 69.
34. Blasse, G. *Proceedings of the International Conference of Magnetism.* Institute of Physics and the Physical Society: London. **1964,** p. 350.
35. Ferguson, J.; Wood, D. L.; Knox, K. *J. Chem. Phys.* **1963,** 39, 881.
36. Ferguson, J.; Knox, K.; Wood, D. L. *J. Chem. Phys.* **1961,** 35, 2236.
37. Lyon, W. G., Ph.D. Thesis, The University of Michigan, Ann Arbor, Michigan **1973.** *Diss. Abs.* **1974,** 35, 74–15790.
38. Shannon, R. D.; Vincent, H. Interatomic Distances and Magnetic properties in halides and chalcogenides. In *Structure and Bonding* 19. Dunitz, J. D.; Hemmerich, P.; Holm, R. H.; Ibers, J. A.; Jorgensen, C. K.; Neilands, J. B.; Reinen, D.; Williams, R. J. P., editors. Springer-Verlag: New Yorк. **1974.**
39. Reynolds, M. L.; Hayston, W. F.; Garlick, G. F. *Phys. Status Solidi* **1968,** 20, 735.
40. Atsarkin, V. A.; Morshnev, S. K.; Potkin, L. I. *Soviet Physics—Solid State* **1967,** 9, 660.
41. Zvyagin, A. I.; Khats'ko, E. N. *Soviet Plastics—Solid State* **1969,** 10, 2970.
42. Bates, C. A.; Oglesby, M. J.; Standley, K. J. *J. Phys. C.* **1972,** 5, 2949.
43. Galkin, A. A.; Prokhorov, A. D.; Tsintsudze, G. A. *Soviet Plastics—Solid State* **1970,** 12, 1414.
44. See for example Lewis, G. N.; Randall, M. *Thermodynamics* revised by Pitzer, K. S.; Brewer, L., editors, second edition. McGraw-Hill Book Co., Inc.: New York. **1961,** chapter 27.
45. Stout, J. W. *Pure Appl. Chem.* **1961,** 2, 287.
46. Mannheim, P. D.; Simopoulos, A. *Phys. Rev.* **1968,** 165, 845; and Nussbaum, R. H.; Howard, D. G.; Nees, W. L.; Steen, C. F. *Phys. Rev.* **1968,** 173, 653.
47. Stout, J. W.; Catalano, E. *J. Chem. Phys.* **1955,** 23, 2013.
48. Schroecke, H. *Neus. Jahrb. Mineral., Abhand.* **1969,** 110, 115.
49. O'Hara, S.; McManus, G. M. *J. Appl. Phys.* **1965,** 36, 1741.
50. Ziman, J. M. *Principles of the Theory of Solids.* Cambridge University Press: Cambridge, England. **1969,** p. 63.
51. Srivastava, K. G. *Phys. Lett* **1963,** 4, 55.
52. Breed, D. J. *Phys. Lett.* **1966,** 23, 181.
53. Akimitsu, J.; Ishikawa, Y.; Endoh, Y. *Solid State Commun.* **1970,** 8, 8187.
54. Goodenough, J. B.; Stickler, J. J. *Phys. Rev.* **1967,** 164, 768.